Available online at www.sciencedirect.com
ScienceDirect
Scripta Materialia 59 (2008) 603–606
Scripta MATERIALIA
www.elsevier.com/locate/scriptamat

Plastic deformation of a Co-based metallic glass composite with in situ precipitated dendritic phases

Jitang Fan,[a] Zhefeng Zhang,[a,*] Baolong Shen[b] and Scott X. Mao[a,c]

[a]*Shenyang National Laboratory for Materials Science, Institute of Metal Research, Chinese Academy of Science, 72 Wenhua Road, Shenyang 110016, China*

[b]*Ningbo Institute of Materials Technology and Engineering, Chinese Academy of Sciences, Ningbo 315201, China*

[c]*Department of Mechanical Engineering, University of Pittsburgh, Pittsburgh, PA 15261, USA*

Received 28 December 2007; revised 13 May 2008; accepted 13 May 2008
Available online 24 May 2008

A new $Co_{43}Fe_{20}Ta_{5.5}B_{31.5}$ metallic glass matrix composite was cast with in situ precipitated crystalline dendrite phases. This composite has particular plasticity properties with a large stress rise after yielding under uniaxial compressive test, which offsets the strength loss, together with local shear deformation and plastic flow within the vein-like structure. In addition, some shear bands – also with the vein-like structure – are observed ahead of the cracks. This indicates that the local shear deformation is triggered by the local shear softening mechanism.

Keywords: Cobalt; Metallic glasses; Composites; Shear bands; Plastic deformation

Enhancing the toughness of materials, by improving their strength and plasticity, is an important area of research. In general, conventional crystalline materials have good ductility, but lack strength. Therefore, on the one hand, scholars have employed a wide range of methods to strengthen conventional materials, e.g. alloying, solid solution, precipitation, dispersion and work-hardening. In addition, controlling the defect density or grain size has also been used as a means to strengthen metallic materials, leading to the production of ultrafine-grained and nanostructured materials [1,2]. On the other hand, many investigators have been trying their best to exploit new alloys with high strength by disordering the crystal lattice so as to forbid the occurrence of slip deformation on the crystallographic planes; this approach has resulted in the birth of amorphous alloys or metallic glasses [3]. In the past two decades, various bulk metallic glasses (BMGs) have attracted particular attention due to their excellent mechanical, physical and chemical properties [4,5]. One significant finding is that the historical record for the strength level of BMG materials has been broken continuously. For example, the strength is in the range of 1500–2000 MPa for Zr-based BMGs [6–8], 1700–2100 MPa for Ti-based BMGs [9], 1900–2500 MPa for Cu-based BMGs and 2700–3100 MPa for Ni-based BMGs [10,11]. In addition, when these amorphous alloys were made into ribbon and wire with a thickness/diameter of about 20 μm, their highest tensile strength was reported to be 3600 MPa for amorphous Fe-based alloy [12], 3580 MPa for amorphous Co–Si–B and 4000 MPa for amorphous Co–Ta–Si–B alloy [13]. Many investigations have also been devoted to improving the plasticity of BMGs. The ductility of these composites has been improved by adding elements with high melting points, such as Ta, Nb or Mo, to Zr-, Cu- and Ti-based BMGs by in situ precipitation of ductile micrometer-sized particles [14,15], body-centered cubic (bcc) β dendrites [16,17] or nanostructured dendrites [18,19] upon cooling from the melting state. It is noteworthy that the strength has recently been improved to a historical peak of about 5300 MPa for Co–Fe–Ta–B amorphous alloy [20]. The plasticity, however, always becomes very bad even in a zero-plasticity fracture with a fragmentation mode [21]. Therefore, this gives rise to the scientifically important problem of how to make Co–Fe–Ta–B amorphous alloy ductile by controlling the microstructure to produce a new material with a super-high strength in combination with certain ductility. In this work, we successfully cast the $Co_{43}Fe_{20}Ta_{5.5}B_{31.5}$ metallic glass composite with a

* Corresponding author. Tel.: +86 24 23971043; e-mail: zhfzhang@imr.ac.cn

1359-6462/$ - see front matter
doi:10.1016/j.scriptamat.2008.05.017

ductile dendritic phase by in situ precipitation. This material displays a slight plastic strain under compressive test, as well as local shear deformation, to form vein-like structure on the fracture surface. Meanwhile, based on the experimental results, we also compare the mechanical properties of the BMG with those of the fully amorphous alloy. Significantly, we introduce a composite material: Co-based BMG composite with a ductile dendritic crystalline phase, which has great potential to be developed into a high-performance material with both high strength and good plasticity.

Multicomponent Co-based alloy ingots with a nominal composition of $Co_{43}Fe_{20}Ta_{5.5}B_{31.5}$ (at.%) were prepared by arc melting mixtures of ultrasonically cleaned Co, Fe and Ta metals with a purity of 99.9% or better and pure crystalline B (99.5 mass%) in a Ti-gettered high-purity argon atmosphere. Bulk alloys in rod form 2 mm in diameter were produced by an ejection copper mold casting method. The as-cast microstructures and the dendritic phase were analyzed by X-ray diffraction (XRD) using a Rigaku diffractometer with CuKα radiation as the source. The sample was etched by hydrofluoric acid in order to expose the dendritic phase and then examined by scanning electron microscopy (SEM) using a Quanta 600. Finally, three samples were tested using a computed-controlled, servohydraulic Instron-8810 testing machine at a strain rate of about $10^{-4}\ s^{-1}$ at room temperature, and the results were averaged to give the final compressive mechanical properties. The deformation and fracture morphologies on the side surfaces and the fractographies were observed by SEM.

Figure 1 shows the XRD diffraction pattern taken from the cross-section surfaces of the as-cast $Co_{43}Fe_{20}$-$Ta_{5.5}B_{31.5}$ alloy rod. It can clearly be seen that the XRD pattern is composed of a broad diffusion background and a set of several sharp crystalline peaks, which correspond to a mixture of the metallic glass matrix and some precipitated crystalline phase, identified as a complex face-centered cubic (fcc) $(Co,Fe)_{21}Ta_2B_6$ phase with a large lattice parameter of 1.055 nm, similar to earlier reports [22,23]. No other crystalline phases could be detected within the sensitivity limits of the XRD. At the same time, the inset of Figure 1 shows the SEM backscattered micrograph of the as-cast alloy etched on the cross-sectional surface, it is interesting to find that the precipitated crystalline phase is clearly dispersed in the metallic glass matrix with some snow-like dendrites. Moreover, there is no any trace of the thick reaction layer at the interface between the precipitated crystalline phase and the metallic glass matrix. Furthermore, neither pores nor voids appear over the whole cross-section of the samples.

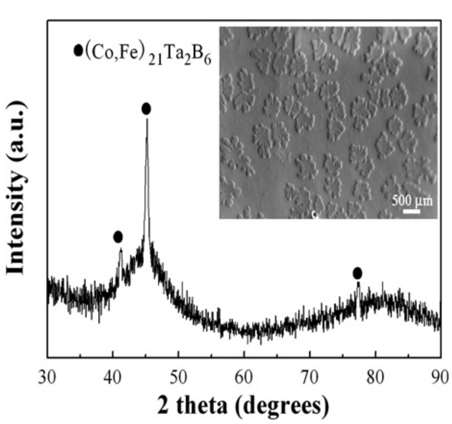

Figure 1. XRD diffraction pattern taken from the cross-section surfaces of the as-cast $Co_{43}Fe_{20}Ta_{5.5}B_{31.5}$ alloy rod. And the inset shows the SEM backscattered electron micrograph of the ductile dendritic crystalline phases on the etched cross-sectional surfaces.

Figure 2 shows one of the engineering stress–strain curves of the as-cast $Co_{43}Fe_{20}Ta_{5.5}B_{31.5}$ alloy with a common aspect ratio (height/diameter = 2), subjected to a uniaxial compressive test at a strain rate of $1 \times 10^{-4}\ s^{-1}$. The specimen displays an initial elastic deformation behavior with an elastic strain of about 1.8%, and then begins to yield at about 4.05 GPa, followed by a large stress rise up to 4.95 GPa with a compressive plastic strain of about 0.4%. Its Young's modulus, E, is about 222 GPa. The compressive mechanical properties for fully amorphous $Co_{43}Fe_{20}Ta_{5.5}B_{31.5}$ alloy were reported in Ref. [20], and are listed in Table 1. Strikingly, for the identical alloy composition under the same compressive conditions, the achievement of 0.4% plastic strain will reduce the yield strength by about 22% and the fracture strength by about 4%. That is, the change of microstructure from fully amorphous to the composite with the precipitated crystalline phase resulted in a decrease in the yield and fracture strength, but contributed to an increase in the plasticity. Furthermore, by comparing the data in Table 1, it can be seen that although it is hard to greatly enhance the plasticity of the amorphous alloy, the increase in the plasticity only leads to a slight loss of strength. Due to the effect of the in situ precipitated dendritic crystalline phase, the alloy begins to yield,

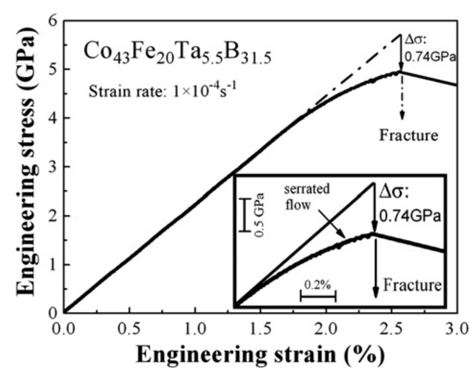

Figure 2. Engineering stress–strain curve of the as-cast $Co_{43}Fe_{20}$-$Ta_{5.5}B_{31.5}$ alloy rod, subjected to uniaxial compressive testing at a constant strain rate of $1 \times 10^{-4}\ s^{-1}$; the inset shows a close-up, displaying serrated flow behavior.

Table 1. The compressive mechanical properties of the current $Co_{43}Fe_{20}Ta_{5.5}B_{31.5}$ alloy and the data reported in Ref. [20]

Alloy	Compressive mechanical properties					
	E (GPa)	σ_y (GPa)	σ_F^C (GPa)	ε_e (%)	ε_p (%)	H/D
Amorphous	268	5.18	5.18	1.9	0	2
Composites	222	4.05	4.95	1.8	0.4	2

showing as the stress–strain curve deviating away from the straight line. The curve continues to show a large stress rise, owing to the super-high strength of the metallic glass matrix. As shear bands propagate, the curve also displays a slightly serrated flow behavior, shown in the inset of Figure 2. Meanwhile, the crystalline phase itself might deform, in company with the metallic glass matrix. Therefore, the high stress rise offsets the loss of strength, leading to a strength loss, $\Delta\sigma$, of only about 0.74 GPa if the alloy still deforms in an ideal elastic way, as shown in Figure 2.

In addition, Figure 3 shows the SEM micrographs of the $Co_{43}Fe_{20}Ta_{5.5}B_{31.5}$ alloy. The image of the etched as-cast alloy shows that the bright phases, corresponding to dendrites with a complex fcc structure, are dispersed homogeneously in the metallic glass matrix, as shown in Figure 3a and in the inset of Figure 1. The dendritic structure processes the character of primary dendrite axes with a length range of 10–20 μm. Furthermore, a regular pattern of secondary dendrite arms with a submicron space of 0.3–3 μm was observed, and even some dendrite arms in nanoscale were also found in Figure 3a. In addition, some parallel shear bands, approximately along the crack, can be observed on the surface, corresponding to the plastic strain (Fig. 3b) [24,25]. Further observations show that a mass vein-like structure appeared at the local region with a clear shear trace, which is a typical feature of the fracture surfaces of ductile metallic glass material with a small ratio of shear strength to cleavage strength, α ($\alpha = \tau_0/\sigma_0$) [26]. This vein-like structure extends along a uniform direction, corresponding to the direction of shear deformation (Fig. 3c), which is similar to previous reports [27–29]. That implies a local plastic deformation, which is in agreement with the shear bands on the surface shown in Figure 3b, contributing to the plastic strain of 0.4% under the compressive test. Furthermore, the slightly enlarged photo shows that most of the vein-like structures consist of melted liquid, flowing along the shear direction. This observation is similar to that on the fracture surface of ductile metallic glass material [26], indicating the occurrence of melting behavior at the moment of fracture. This also further illustrates the increase in the temperature inside the material, due to the super-high elastic energy (Fig. 3d). Moreover, some vein-like patterns appear in the gaps between the cracks (Fig. 3e). This implies that the melting behavior not only took place on the surface, but also appeared in the gaps between the cracks, probably due to the temperature rise inside the shear bands [30]. Those observations provide indirect evidence for the local shear strain. In addition, some shear bands were also observed at the tip of crack, together with the vein-like structure too (Fig. 3f). This implies that the shear deformation happened as a result of the local shear softening mechanism in the fracture process [31], which corresponds to the slight global plasticity.

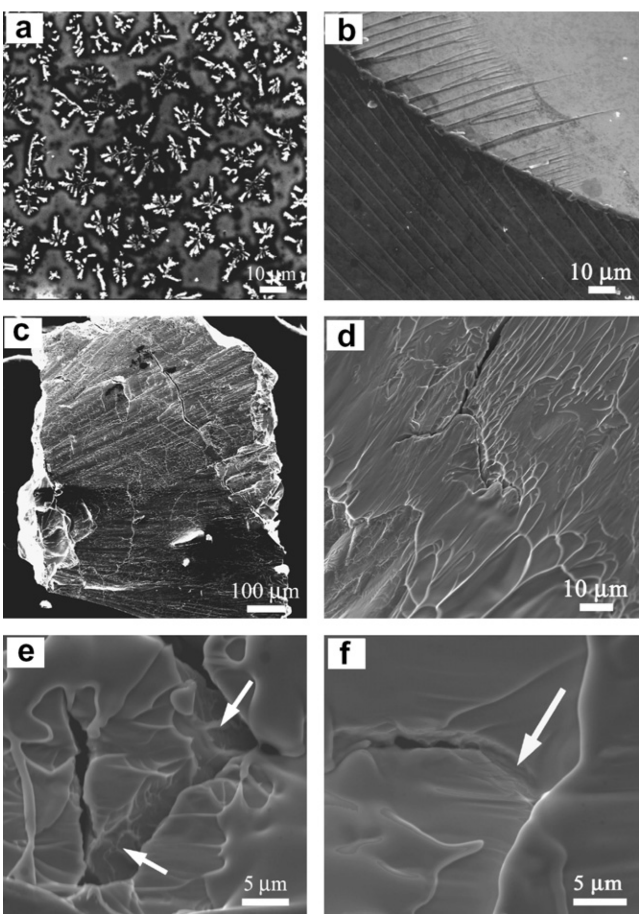

Figure 3. SEM fractographies of the $Co_{43}Fe_{20}Ta_{5.5}B_{31.5}$ alloy after compressive fracture. (a) Precipitated crystalline phase with a dendritic pattern: $(Co,Fe)_{21}Ta_2B_6$; (b) shear bands on the surface; (c) fracture surface induced by shear deformation with melted vein-like structure; (d) melted liquid with a large plastic flow; (e) vein-like structure in the gap of crack; and (f) shear bands at the tip of the crack, suggesting a local shear deformation.

In summary, we report that the $Co_{43}Fe_{20}Ta_{5.5}B_{31.5}$ alloy can be successfully cast into a new composite with a metallic glass matrix and some in situ precipitated dendritic phases. It shows a plastic strain of about 0.4% with a large stress rise of about 0.9 GPa under uniaxial compressive test, along with local shear deformation and plastic flow, displaying some local shear bands and vein-like patterns on the fracture surface. Meanwhile, by comparing the mechanical properties of this composite with those of the fully amorphous alloy, it is noted that enhancing the plasticity only results in a slight strength loss, due to the precipitation of dendritic crystalline phases. Therefore, this Co-based metallic glass composite can be considered to have potential to be developed into a high-performance material with both high strength and good plasticity.

The authors acknowledge the financial support of the National Natural Science Foundation of China (NSFC) (Grant No. 50401019), the “Hundred of Talents Project” from the Chinese Academy of Science and the National Outstanding Young Scientist Foundation for Z. F. Zhang (Grant No. 50625103).

[1] R.Z. Valiev, R.K. Islamgaliev, I.V. Alexandrov, Progress in Materials Science 45 (2000) 103.
[2] H. Gleiter, Acta Materialia 48 (2000) 1.
[3] W. Klement, R.H. Willens, P. Duwez, Nature 187 (1960) 869.
[4] W.L. Johnson, MRS Bulletin 24 (1999) 42.

[5] C.A. Schuh, T.C. Hufnagel, U. Ramamurty, Acta Materialia 55 (2007) 4067.
[6] A. Peker, W.L. Johnson, Applied Physics Letters 63 (1993) 2342.
[7] A. Inoue, T. Zhang, Materials Transactions JIM 36 (1995) 1184.
[8] J.T. Fan, F.F. Wu, Z.F. Zhang, F. Jiang, J. Sun, S.X. Mao, Journal of Non Crystalline Solids 353 (2007) 4707.
[9] Y.C. Kim, S. Yi, W.T. Kim, D.H. Kim, Materials Research Society Symposium Proceedings 644 (2001) L4.9.1.
[10] A. Inoue, W. Zhang, T. Zhang, K. Kurosaka, Acta Materialia 49 (2001) 2645.
[11] T. Zhang, A. Inoue, Materials Transactions 43 (2002) 708.
[12] B.L. Shen, A. Inoue, C.T. Chang, Applied Physics Letters 85 (2004) 4911.
[13] M. Hagiwara, A. Inoue, T. Masumoto, Materials Science and Engineering A 54 (1982) 197.
[14] C. Fan, R.T. Ott, T.C. Hufnagel, Applied Physics Letters 81 (2002) 1020.
[15] J.C. Lee, Y.C. Kim, J.P. Ahn, H.S. Kim, S.H. Lee, B.J. Lee, Acta Materialia 52 (2004) 1525.
[16] C.C. Hays, C.P. Kim, W.L. Johnson, Physical Review Letters 84 (2000) 2901.
[17] Z. Bian, H. Kato, C.L. Qin, W. Zhang, A. Inoue, Acta Materialia 53 (2005) 2037.
[18] G. He, J. Eckert, W. Loser, L. Schultz, Nature Materials 2 (2003) 33.
[19] U. Kuhn, J. Eckert, N. Mattern, L. Schultz, Applied Physics Letters 80 (2002) 2478.
[20] A. Inoue, B.L. Shen, H. Koshiba, H. Kato, A.R. Yavari, Acta Materialia 52 (2004) 1631.
[21] Z.F. Zhang, H. Zhang, B.L. Shen, A. Inoue, J. Eckert, Philosophical Magazine Letters 86 (2006) 643.
[22] P. Villars, L.D. Calvert, in: L. Kacprzak (Ed.), Pearson's Handbook of Crystallographic Data for Intermetallic Phases 2 (1991) 1428.
[23] M. Imafuku, S. Sato, T. Nakamura, H. Koshiba, E. Matsubara, A. Inoue, Materials Research Society Symposium Proceedings 644 (2001) L1.6.1.
[24] J.J. Kim, Y. Choi, S. Suresh, A.S. Argon, Science 295 (2002) 654.
[25] J. Schroers, W.L. Johnson, Physical Review Letters 93 (2004) 255506.
[26] Z.F. Zhang, J. Eckert, Physical Review Letters 94 (2005) 094301.
[27] P.E. Donovan, Acta Materialia 37 (1989) 445.
[28] A. Leohard, L.Q. Xing, M. Heilmaier, A. Gebert, J. Eckert, L. Schulta, Nanostructured Materials 10 (1998) 805.
[29] G. Subhash, R.J. Dowing, L.J. Kecskes, Materials Science and Engineering A 334 (2002) 33.
[30] J.J. Lewandowski, A.L. Greer, Nature Materials 5 (2006) 15.
[31] X.K. Xi, D.Q. Zhao, M.X. Pan, W.H. Wang, Y. Wu, J.J. Lewandowski, Physical Review Letters 94 (2005) 125510.